


Article

# Cooperative SWIPT THz-NOMA/6G Performance Analysis

Haider W. Oleiwi \*  and Hamed Al-Raweshidy

Department of Electronic and Electrical Engineering, Brunel University London, London UB8 3PH, UK; Hamed.Al-Raweshidy@brunel.ac.uk

\* Correspondence: Haider.Al-Lami@brunel.ac.uk

**Abstract:** In this paper, cooperative simultaneous wireless information and power transfer terahertz (THz)-nonorthogonal multiple access (NOMA) is considered to overcome the challenging shortages that THz communications have due to THz characteristics. The proposed system presents a noticeable improvement in energy efficiency (EE) and spectral efficiency (SE), in addition to other important metrics. By utilizing NOMA technology and THz frequencies, it aims to improve connectivity, resource management, SE, reliability, scalability, user fairness, and to enhance the overall performance of wireless communications. Accordingly, the outcome shows how the introduced energy harvesting technique manages to improve EE and SE compared with the conventional cooperative networks of the recent related work (e.g., cooperative MIMO-NOMA with THz) by 70%. The author also minimizes the transmission power and maximizes the EE by using a decode-and-forward relay rather than an intelligent reflecting surface, which aims to reduce the dissipation in the transceiver hardware, computational complexity, and improves reliability and transmission rate.

**Keywords:** 6G; cooperative networks; energy efficiency; energy harvesting; NOMA; outage probability; resource management; SWIPT; spectral efficiency; THz



Citation: Oleiwi, H.W.;

Al-Raweshidy, H. Cooperative SWIPT THz-NOMA/6G Performance Analysis. *Electronics* **2022**, *11*, 873. <https://doi.org/10.3390/electronics11060873>

Academic Editor: Nurul I. Sarkar

Received: 7 February 2022

Accepted: 9 March 2022

Published: 10 March 2022

**Publisher's Note:** MDPI stays neutral with regard to jurisdictional claims in published maps and institutional affiliations.



**Copyright:** © 2022 by the authors. Licensee MDPI, Basel, Switzerland. This article is an open access article distributed under the terms and conditions of the Creative Commons Attribution (CC BY) license (<https://creativecommons.org/licenses/by/4.0/>).

## 1. Introduction

The tremendous growth of service-demanding smart devices, e.g., global coverage, unprecedented technologies, and intelligent applications accompany the rapid leap in wireless communications. Necessary data transfer with ubiquitous coverage led to revolutionary research efforts. Energy efficiency (EE) and spectral efficiency (SE) are sharp criteria that measure the compatibility of any proposed system [1–4]. Their improvement is essential to meet the stringent requirements of various applications, such as data-hungry and energy-demanding applications, due to 6G increasing demands with its key-enabling technologies. EE is considered a crucial designing metric in wireless communications, particularly in 6G and beyond with their upgraded infrastructures, such as cell-free and ultra-dense heterogeneous networks (UDHNs) with distributed base stations, access points, and relays due to their number of antennas, equipment, and power-consuming electronic (and photonic) elements, connecting billions of devices, i.e., Internet of Everything (IoE) [5–10]. The EE of 6G operations is compulsory for energy savings, green communications, and feasibility in 6G network requirements such as quality of service (QoS) and processing [11]. Terahertz (THz) communication [12] is a cornerstone that will play a pivotal role in the next generations. SE depends mainly on available channel bandwidth (BW) following Shannon's theorem. THz has attracted the great attention of many researchers as the hottest topic in the paradigm shift of 6G due to its unique advantages as the last uninvestigated band of electromagnetic frequencies. It is in the middle of millimeter Wave (mmWave) and infrared bands between (0.1–10) THz and is considered the system's backbone of the next era due to its ability to enable various applications. THz communication has extremely high frequencies, ultrawide BW, superfast data transfer, extensive throughput, extremely low latency, and very good directivity due to its very short wavelength (3–0.03) mm. Locating the boundary between mmWave and optical bands motivated researchers to explore these

bands' capability to support THz communications as THz outperforms the two bands at specific points. Electronic, photonic, and plasmonic technologies are expected to evolve the manufacturing of THz transceivers. THz communication is logically complementing mmWave and optical bands by providing alternative signals as a replacement to optical paths in some use cases, such as the connections of backhaul, kiosk to nodes, data center's racks, and intra-device links, in addition to THz integration with fiber networks [13]. Hence, the disadvantage of noticeable water vapor absorption and path loss spikes that divide the THz spectrum into several spectral windows, as stated in IEEE Std. 802.15.3d-2017; however, these windows are being extensively explored, considering them to support 6G services with some exemptions where some 6G services will not be compatible with the new frequency bands [14]. The demand for IoE ignites an emergent necessity to connect everything to everything. The current systems have limitations that restrict any upgrades or improvements to meet these requirements. Developing decent techniques to be integrated altogether is mandatory to build a modern communication system in order to satisfy the new requirements such as ultra-massive connectivity, very high SE, very low latency, very high data rate, ultra-high reliability, user fairness, supporting unprecedented applications, EE, and cost-effectiveness. Power domain nonorthogonal multiple access (NOMA) [15] is one of the famous candidates to evolve 6G systems. It can improve the SE of mobile communication systems, outperforming conventional orthogonal multiple access (OMA) schemes in terms of SE, capacity, resource allocation, user fairness, connectivity, and latency. Our research mainly concentrates on single-input single-output (SISO)-NOMA (despite the gains of multiple-input multiple-output (MIMO) systems) because MIMO-NOMA systems are practically complicated to implement. NOMA mechanism allows various users' signals to superimpose at the transmitter (Tx) and then to be distinguished and filtered by using successive interference cancellation (SIC) operation at the receiver (Rx) that effectively enlarges the data transfer capacity that depends mainly on the BW; however, interference is discarded by the SIC implementation, and the noise is filtered. The two operations are conducted at the Rx side. With the NOMA concept, the channel capacity is calculated as  $C = BW \times \log_2(1 + S/(N + I))$ , where  $C$  is the channel capacity,  $BW$  is the bandwidth,  $S$  is the signal power,  $N$  is the noise power, and  $I$  is the interference of other users' signals. NOMA multiplexing is performed in the power domain, allocating different power coefficients to the users per their channel conditions (i.e., good or bad). All users' signals are superimposed in Tx. Demultiplexing of NOMA signals is conducted by applying SIC at Rx. Grouping or clustering the served users is essential in THz-NOMA communications to improve SE and mitigate complexity as the line-of-sight (LOS) is the main transmission link. For the NOMA-SISO scheme, BS/users with single antenna equipment rely on the simultaneous channel state information (CSI), where the users are sorted to allow decent SIC decoding at Rx. The larger the channel gain difference, the more sufficient NOMA we gain. User clustering may be impractical with many users; therefore, we aim to develop low complexity solutions to avoid the clustering problem [16,17]. SIC is not only CSI-based but also QoS-based or hybrid-based [16]. CSI acquisition at Tx and Rx is a great challenge for all modulation schemes [14].

Hence, we use simple binary phase-shift keying (BPSK) in our system with its advantages compared with other formats. Research efforts are exploring all the possible means, including NOMA-assisted cooperative systems, to tackle the problems of distance shortages and power losses in THz communications. Cooperative networking with its relaying categories offers multiple advantages such as reliability and capacity with better coverage area, enhancing overall performance. When applied to cooperative networks, the SE of NOMA can be reasonably improved to support extra (blocked, weak, or cell-edge) users in the short-distance THz transmission, significantly when deploying energy harvesting (EH) with NOMA-based cooperative networks [18]. It represents the main topic of our paper in THz communications. Hence, we use decode-and-forward (DF) relaying because NOMA is adopted in our system. Relaying user implies a copy of the far (weak) users' signal (to decode and remove it before decoding the intended strong user's signal in NOMA) in-

cluded in the superposed signal received by that user. We reasonably utilize that to achieve the objective of relaying as an additional advantage, which is better than using an extra relaying device with extra costly power-consuming complexity. The repetitive use of cooperative networks causes the drainage of the relaying user's battery, leading to system failure because THz-NOMA requires high computational SIC procedures at the Rx. Thus, research efforts aim to overcome the challenge of moving toward green communications [19] by applying the EH technique. Energy and information are sent to other destinations by exploiting the energy of radiofrequency (RF) signals that exist everywhere around most devices. EH enables devices to harvest that energy by using simple RF circuits. We can then utilize that harvested power to use it again with our transmissions to send our signals without applying an extra burden to the relaying user's battery. Relaying user divides the received signal's power into EH and information decoding through EH power splitting, allowing the implementation of energy harvesting and information decoding at the same time, leading to the principle of simultaneous wireless information and power transfer (SWIPT). SWIPT qualifies the near-relaying user to capture power from the transmitted signal from the source and uses that energy to relay information to the far user, as shown in Figure 1 [18]; this improves the system throughput and outage probability accordingly.

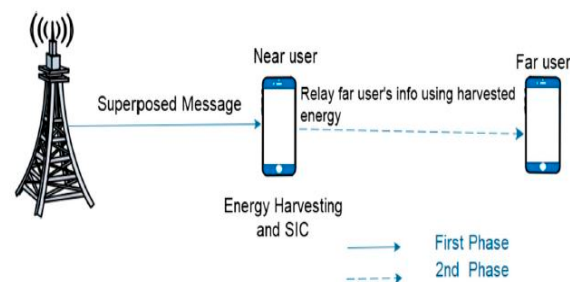


Figure 1. SWIPT with cooperative NOMA.

The rest of this paper is arranged as follows. Section 2 explains several recent studies with their achieved goals. The contributions of this paper are presented. Section 3 discusses our system model by deriving the closed-forms based on IEEE Standard 802.15.3d/2017 parameters and providing the benefits of using such a system with the promising technologies to produce a decent wireless system for THz communications for improving the consistency of networks and the performance of communication, showing the needs behind the introduction of such energy-efficient system. Sections 4 and 5 conduct mathematical analysis and simulations for comparison. We simulate our system by discussing the outcome and how those results present an added value to the current systems. A discussion is presented on the basis of improving the overall performance of THz-NOMA networks under resource availability, showing the main differences in performance when using different distances with each part of this network separately, and showing the outperformance of using DF-Relayed SWIPT THz-NOMA system over the previous systems. Sections 6 and 7 address the challenges and summarize the conclusion, respectively.

## 2. Related Works

Cooperative networks were studied with many use cases and scenarios, where the main benefits were fully demonstrated, addressing the disadvantages of using that technique with wireless communication systems. Similarly, for other technologies of this paper, that is, EH, NOMA, and THz communications, each technology is considered either separately or by integrating some of them to achieve a particular impact on the wireless communication field. The disadvantages of using any of the mentioned technologies were discussed thoroughly, showing the weak points, limitations, and the shortage of performance throughout the research attempts by academic and industrial research centers.

In [19,20] as shown in Figure 2 in THz communications, although the intelligent reflecting surface (IRS) technique is regarded as a promising technology to enhance the

connectivity between Tx and the shadowing Rx in specific scenarios (disconnected or weak signal users), it still needs to aggregately outperform the use of relaying systems of cooperative networks in terms of complexity, power consumption, and cost-effectiveness, by concentrating on optimizing reflection process and considering all the calibrating metrics. This introductory study briefly compares IRS technology with the old DF relaying. The first perception of this study is that the very high rates with/without IRS are required to surpass DF relaying in terms of minimizing the transmission power and maximizing EE in addition to the extra equipment hardware.

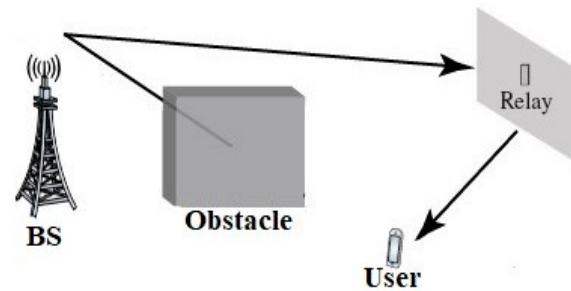


**Figure 2.** Relay-assisted transmission.

In [14], the authors presented some significant points as drawbacks or difficulties against designing and deploying IRS technique for supporting 6G infrastructure, that is, controlling the alignment of beams for instantaneous beam steering, interference control, energy efficiency degradation, and the challenges that accompany IRS deployment, such as the (1) design and control joint communications of active and passive components, for instance, extra operations and analyses needed, which is about improving the PHY coverage and hardware effects on the performance, in addition to the total cost of renting a space to deploy it and the continuous maintenance needed. (2) Effect of potential full or partial failures due to environmental or accidental factors, such as temperature, rain, and wind. (3) IRS standardization before system deployment and the interactivity of IRS with the radio traffic instant changes to attain efficient signaling. (4) The computational and procedural complexity as additional transmission steps.

The authors in [21] studied clustering, precoding, and power optimization. They proposed a new scheme for clustering in THz MIMO-NOMA designs by developing an artificial intelligent K-means algorithm. In [22], a widespread MIMO spatial multiplexing technique using a new index modulation range is proposed with MIMO technique at sub-THz frequencies studied to develop ultra-high data rate applications, achieving high SE. In [23], the authors studied the power allocation problem in cooperative THz MIMO-NOMA systems in half-duplex and full-duplex modes to maximize users' achievable rates.

To the best of the authors' knowledge, EH (SWIPT) has not been applied to cooperative THz-NOMA systems yet. Its SE and EE have not been investigated. The main contributions of this paper are as follows:

- (1) We briefly study the use of DF relaying rather than complex and costly IRS for cooperative networking to achieve the same goal of reliable connectivity with non-LOS (NLoS) transmission path in THz frequencies for open terrestrial areas, such as rural areas, countryside, or any area where we cannot deploy IRS (assuming the existence of an obstacle blocking the transmission path) or for low-rate communication use cases in a new potential system.
- (2) We investigate system performance when applying the EH SWIPT technique for enhancing THz transmission.
- (3) We enhance SE, EE, and other metrics compared with previous studies by integrating THz, NOMA, cooperation, and EH technologies.
- (4) We propose a simple and cost-effective design of SISO high-directional antenna with the system to simplify THz-NOMA networks and not MIMO (this design reduces decoding

- complexity at Rx where we do not need extra SE while using THz and NOMA) and to reduce bulky hardware, computational complexity, power consumption, and cost.
- (5) We suggest using a relaying node rather than a dedicated relaying device to gain an extra served user, considering the flexibility.
  - (6) We propose two-user clustering to avoid complexity and SE degradation due to signals' added headers to overcome error propagation in SICs.
  - (7) We analyze our scalable system and simulate performance while setting moderate and flexible parameters (i.e., distances, transmission power, frequency, BW, and simple modulation scheme as we do not need to use a complex modulation to improve SE). This system is upgradeable based on trade-offs among systematic priorities.
  - (8) We demonstrate the importance of selecting the nearest relaying user to the Bs based on those technologies' concepts.

### 3. System Model

The proposed simple system in Figure 3 can work in a terrestrial open space use case, where THz-NOMA smallest single-cell downlink transmission with a cluster of two paired users is considered. The BS implements superposition to send signals to the two users simultaneously near user (NU) and far user (FU) by using SISO with a high-directional antenna. An obstacle is located in the path between BS and FU, causing extreme shadowing. Thus, the FU is not capable of detecting its blocked or weak signal; however, NU has a strong connection with the BS. Under NOMA fundamentals, firstly, FU's signal must be decoded by NU before performing SIC to remove it and consequently decode NU's data. Thus, NU already has a copy of the FU's information. Accordingly, NU can assist FU's connection by playing the role of DF relay; however, the NU battery's energy does not suffice to relay the information to the FU. For that purpose, we proposed NU to perform the power-splitting protocol of EH (SWIPT) to capture power from BS and RF energy surrounding NU. The entire transmission process is performed in two stages. In the first stage, NU receives the transmitted signal from BS.

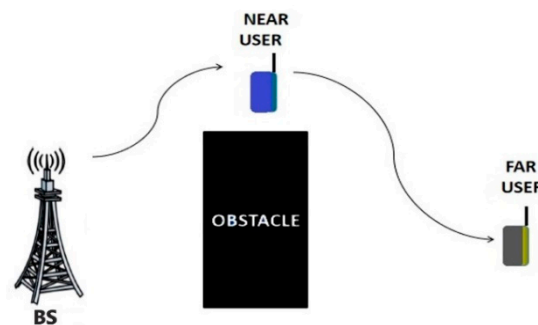


Figure 3. Model of cooperative SWIPT THz-NOMA.

An amount of NU's received power will be captured using the power-splitting process, whereas the left power will be exploited to decode data. In the next stage, NU uses the captured power to relay the FU's information to the FU.

The proposed channel model in this paper of all scenarios is Rayleigh fading channel with zero mean and variance = Transmission Distance<sup>-THz total losses</sup>, whereas the transmission noise is additive white Gaussian noise (AWGN) with zero mean and variance =  $\sigma^2$ . The Gaussian distributed probability density function (PDF) of  $z$ -point is expressed as:

$$f_{(z;\sigma)} = \frac{1}{\sqrt{2\pi\sigma^2}} \exp\left(-\frac{z^2}{2\sigma^2}\right) \quad (1)$$

The signal model of cooperative SWIPT NOMA considers atmospheric attenuation and molecular absorption, and the path loss of NLOS is more than that of the LOS path. The NLOS effect can be abandoned if the LOS path dominates [20]. Hence, in the assumed

open space transmission medium, the THz total losses ( $\eta$ ) is set to be extremely high. The channel gain for a  $k$ th number of users can be calculated as

$$h_k = \sqrt{A} \sqrt{\frac{1}{\eta}} G \tag{2}$$

where  $A$  is the number of antennas for SISO,  $G$  is the antennas' gain, and  $\eta$  is the THz total losses between source and destination, given by

$$\eta = \left(\frac{4\pi f d}{C}\right)^2 e^{a(f)d} \tag{3}$$

where  $f$  is the THz frequency,  $d$  is the source to destination distance,  $a(f)$  is the absorption coefficient of the transmission medium, and  $c$  is the speed of light.

The closed forms based on our scenario are derived as follows:

Phase 1: The transmitted superposed signal by Tx is expressed as

$$X = \sqrt{P}(\sqrt{\alpha n} x_n + \sqrt{\alpha f} x_f) \tag{4}$$

where  $P$  is the transmission power,  $\alpha n$  is the NU's power,  $\alpha f$  is the FU's power,  $x_n$  is the NU's power signal, and  $x_f$  is the FU's power signal. The FU cannot receive the signal due to full shadowing. The NU's received signal is expressed as

$$y_n = \sqrt{P}(\sqrt{\alpha n} x_n + \sqrt{\alpha f} x_f) h_{sn} + w_n \tag{5}$$

where  $h_{sn}$  is the BS-NU Rayleigh fading coefficient with zero mean and variance =  $d s n^{-\eta}$ ,  $d s n$  is the BS-NU distance, and  $w_n$  is the AWGN with zero mean and variance =  $\sigma^2$ . From  $y_n$ , NU harvests a fraction of power called the EH coefficient (denoted as  $\psi$ ). The remaining power fraction ( $1 - \psi$ ) is the information decoding power. Accordingly, when energy is harvested, the information decoding signal is

$$y_D = \left(\sqrt{(1 - \psi)}\right) y_n + w_{eh} = \left(\sqrt{(1 - \psi)}\right) \sqrt{P} (\sqrt{\alpha n} x_n + \sqrt{\alpha f} x_f) + \left(\sqrt{(1 - \psi)}\right) w_n + w_{eh} \tag{6}$$

where  $w_{eh}$  is the thermal noise of EH electronic components (mean = 0 and variance =  $\sigma^2$ ). Mathematically, we ignore the harvested power of  $w_n$ , and  $y_D$  will be represented as

$$y_D = \left(\sqrt{(1 - \psi)}\right) \sqrt{P} (\sqrt{\alpha n} x_n + \sqrt{\alpha f} x_f) + w_{eh} \tag{7}$$

From  $y_D$ , NU decodes  $x_f$  directly. NU achievable rate for FU's information decoding is

$$R_{nf} = \frac{1}{2} \log_2 \left( 1 + \frac{(1 - \psi) P \alpha f |h_{sn}|^2}{(1 - \psi) P \alpha n |h_{sn}|^2 + \sigma^2} \right) \tag{8}$$

By performing SIC, NU achievable rate for NU's data decoding is

$$R_{nf} = \frac{1}{2} \log_2 \left( 1 + \frac{(1 - \psi) P \alpha n |h_{sn}|^2}{\sigma^2} \right) \tag{9}$$

Harvested power:  $\psi$  is the EH coefficient captured in the first stage. The harvested energy is expressed as

$$PH = P |h_{sn}|^2 \zeta \psi \tag{10}$$

where  $\zeta$  is the circuitry EH efficiency.

Phase 2: In the second stage, *NU* relays the information that is intended for the *FU* by using the harvested energy (*PH*). Thus, the transmitted signal by the *NU* is

$$\sqrt{PH} \tilde{x}_f \tag{11}$$

The received signal at the *FU* is

$$\sqrt{PH} \tilde{x}_f h_{nf} + w_f \tag{12}$$

where *h<sub>nf</sub>* is the Rayleigh fading channel between *NU* and *FU*. The achievable rate at the *FU* is

$$R_f = \frac{1}{2} \log_2 \left( 1 + \frac{PH|h_{sn}|^2}{\sigma^2} \right) \tag{13}$$

*NU* must decode the *FU*'s data in the first stage to derive an expression for evaluating the optimal value of the power-splitting coefficient  $\psi$ . It will then be able to relay the *FU*'s information appropriately. To achieve that, we set the condition:  $R_{nf} > R_{f*}$ .

Where  $R_{f*}$  is the *FU*'s target rate. This condition assumes that *NU*'s achievable rate for *FU*'s information decoding must surpass *FU*'s target rate.  $R_{nf}$  in Equation (9) in the assumed constraint above is substituted to derive  $\psi$

$$\frac{1}{2} \log_2 \left( 1 + \frac{(1-\psi)P \alpha_f |h_{sn}|^2}{(1-\psi)P \alpha_n |h_{sn}|^2 + \sigma^2} \right) > R_{f*} \tag{14}$$

$$\log_2 \left( 1 + \frac{(1-\psi)P \alpha_f |h_{sn}|^2}{(1-\psi)P \alpha_n |h_{sn}|^2 + \sigma^2} \right) > 2R_{f*} \tag{15}$$

$$\frac{(1-\psi)P \alpha_f |h_{sn}|^2}{(1-\psi)P \alpha_n |h_{sn}|^2 + \sigma^2} > 2^{2R_{f*}} - 1 \tag{16}$$

We denote  $2^{2R_{f*}} - 1$  by  $\tau_f$ , which is *FU*'s target SINR.

$$\frac{(1-\psi)P \alpha_f |h_{sn}|^2}{(1-\psi)P \alpha_n |h_{sn}|^2 + \sigma^2} > \tau_f \tag{17}$$

$$(1-\psi)P \alpha_f |h_{sn}|^2 > \tau_f(1-\psi)P \alpha_n |h_{sn}|^2 + \tau_f \sigma^2 \tag{18}$$

$$(1-\psi)P \alpha_f |h_{sn}|^2 - \tau_f(1-\psi)P \alpha_n |h_{sn}|^2 > \tau_f \sigma^2 \tag{19}$$

$$(1-\psi)P |h_{sn}|^2 (\alpha_f - \tau_f \alpha_n) > \tau_f \sigma^2 \tag{20}$$

$$\psi < 1 - \frac{\tau_f \sigma^2}{P |h_{sn}|^2 (\alpha_f - \tau_f \alpha_n)} \tag{21}$$

To make sure that  $\psi$  is less than that value, we reform the above equation to be

$$\psi = 1 - \frac{\tau_f \sigma^2}{P |h_{sn}|^2 (\alpha_f - \tau_f \alpha_n)} - \delta \tag{22}$$

where  $\delta$  is a tiny number (i.e.,  $10^{-6}$ ) This value of  $\psi$  assures the required power for information decoding to achieve the *FU*'s target rate.

Outage Probability:

The outage probability for each user is the probability of falling the user's instantaneous data rate below the target. Assuming  $R_{n*}$  and  $R_{f*}$  (bits/s/Hz) are *NU*'s and *FU*'s target rates, respectively.

$FU$  will be in an outage if its achievable rate  $Rf$  in (13) is less than the target rate, which is mathematically expressed as

$$PFU = Pr(Rf < Rf^*) \quad (23)$$

$NU$  must decode the  $FU$ 's signal and its own precisely. The target rates for  $NU$  and  $FU$  must reach the  $NU$ 's target rate. With SIC operation, if the target rate of either  $NU$  or  $FU$  in (9) and (13) does not reach  $NU$ 's target rate, then  $NU$  will be in an outage, which is mathematically expressed as

$$PNU = Pr(RNF < Rf^*) + Pr(RNF > Rf^*, Rn < Rn^*) \quad (24)$$

We adopt the first mode principle that is stated in the physical layer section in [24], which is the THz single-carrier. This principle was proposed for high data rate connections, targeting BW-dependent applications, such as wireless backhaul/backhaul links, fronthaul/backhaul links, and data center links [25], based on the availability of spectral windows within THz frequencies (252.72–321.84) GHz. The available spectrum is divided into various channels (approved at World Radio Conference 2019 [WRC-2019]) due to atmospheric and other effects where every individual channel has its characteristics [25]. In total, 69 overlapping channels and 8 supported BWs (2.16–69 GHz) were found as multiples of 2.16 GHz. The widest entire channel (69.12) or the multiple smaller channels might be allocated depending on the application requirements, hardware limits, transmission conditions, and compatibility with the system.

Among various modulation schemes that THz-SC PHY supports, we adopt BPSK as the simplest scheme, although BPSK and QPSK modulations are compulsory. We need to balance the range of distances and the system performance per the use case, application, and deployment, i.e., range–rate trade-off policy [24].

#### 4. Simulation Scenarios

The simulation scenarios are as follows (based on IEEE standard parameters [24]): The first simulation was to demonstrate the validity of using DF relaying rather than IRS for the same purpose to gain the mentioned benefits, and the values of all parameters can be found in [20]. The subsequent simulation was compared with the mathematical analysis. We then simulated the paper's main scenarios. Scenario1: Cooperative SWIPT THz-NOMA using equal distance for two stages ( $BS-NU$  and  $NU-FU$ ) with moderate parameters' values of frequency, BW, power, and distance to compare it with the previous work. Scenario2: same system with an enlarging distance of each stage apart ( $BS-NU$ ,  $NU-FU$ ) changing parameters' values for distance adapting reason to compare the two cases with the main Scenario1 to study the effect of distancing and changed parameters. For the two scenarios, we set: (1) Transmission power, frequency, BW, and distance to be adjustable. (2) Simple target of 1 Gbps as a reference point for comparison. (3) Power (30 dBm) is used with Scenario1 to cover more distance in case of having longer  $FU$ 's distance (it could be 20 dBm or less). Accordingly, 42 dBm power is set with Scenario2 while enlarging distances. (4) High path loss exponent assumed  $\eta = 4$  as a worst-case scenario (while it could be less, such as urban or the best UDN case). The absorption coefficient can be found in [20]. The simulation results are based on the MATLAB program.

#### 5. Simulation Results

In this section, numerical analysis and simulation were implemented to validate the optimized achievable rates and outage probability. Table 1 denotes the simulation parameters.



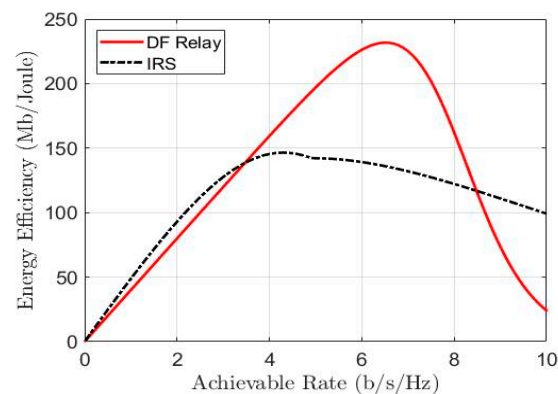
**Table 1.** Simulation parameters.

Parameters	Scenario1	Scenario2
Frequency	311.04 GHz	287.28 GHz
Bandwidth	12.96 GHz	69.12 GHz
Transmission power	30 dBm	42 dBm
Transmission distance	Phase 1 = 10 m Phase 2 = 10 m	(1) Phase 1 = 15 m, Phase 2 = 10 m (2) Phase 1 = 10 m, Phase 2 = 15 m
$NU$ power coefficient	0.2 of total power	
$FU$ power coefficient	0.8 of total power	
Antenna gain	25 dB	
Path loss exponent	4	
Target data rate	1 Gbps	
EH conversion efficiency	0.7	

As mentioned previously, the simulation results validate the derived closed forms of our optimized system. These results are compared with that of previous work, whereas the same system is compared with the suggested Scenario2, changing the metrics of the two cases. The system performance was investigated depending on some parameters that THz communication yields. The proposed mechanism should enable the blocked node to maintain ongoing communication while being on shadowing by BS. The next sections explore the capability of this simple and scalable system to manage the THz transmission shortage, showing how this can improve SE, EE, reliability, and overall performance.

### 5.1. DF Relay vs. IRS

In this section, we present the simulation of DF relay-assisted source to destination connection versus IRS-assisted connection (as shown in Figure 4) to validate the reason behind using such a technique, utilizing its advantages compared with IRS based on the scenario shown in Figure 2 using the SISO technique.

**Figure 4.** EE of DF Relay vs. IRS.

According to the comparison in Figure 4, DF relaying outperforms the new IRS technology (despite its unique advantages) in specific cases, whereas IRS needs a huge number of bulky power-consuming reconfigurable elements to be competitive because of the obtained low channel gain due to the two transmission stages it propagates from source to destination throughout reflection (e.g., IRS needs a place to be deployed in, with continuous maintenance); however, in DF relaying, the signal is transmitted twice with different channel gains. The EE of using DF relay with THz-NOMA, including EH, demonstrates the validity of this system even for very-high-rate communications.

### 5.2. System Numerical Analysis and Simulation

In this section, we manipulate mathematical analysis and simulation of the main system model, exploring the system performance in terms of sum-throughput and outage probability based on the parameters of Scenario1 mentioned in Sections 4 and 5 (with 20 dBm transmit power) to validate our optimized system model analysis, achieving our intended objectives.

Figures 5 and 6 show a notable matching of analytical and simulation results, affirming the precision of our analysis and proving the validity of our system model, gaining the novelty of added values (detailed next section).

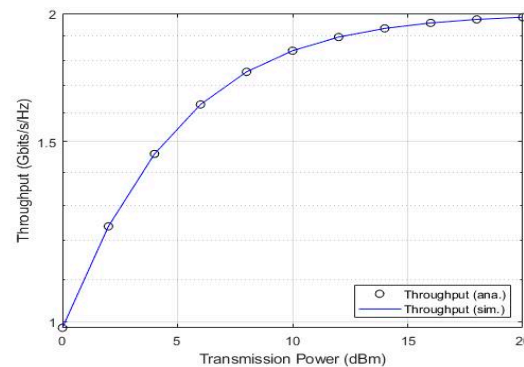


**Figure 5.** Sum-Throughput vs. Transmit Power.

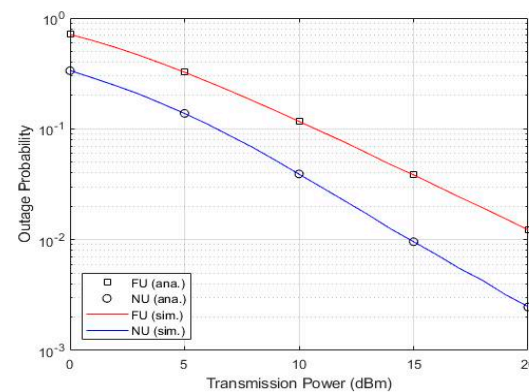


**Figure 6.** Users' Outage Probability vs. Transmit Power.

### 5.3. System Simulation

In this section, we present the simulation of the main system model for every single user in three subsections to study the system performance based on the parameters of Scenario1 mentioned in Sections 4 and 5 to compare it with the similar recent work and to demonstrate how our proposed system presents a valuable enhancement to the wireless communication field using the promising technologies.

#### 5.3.1. Average Achievable Rate against Transmit Power

Figure 7 depicts the performance of users in accordance with allocated power. The *NU* is saturated at 1 Gbps/Hz due to the EH mechanism that uses only the required power to reach the targeted rate and capture all the remaining power, and the *FU* data rate keeps increasing (does not affect *NU* stability) by using the harvested power; however, we can exploit the overused power of the *FU* for more EH operations.

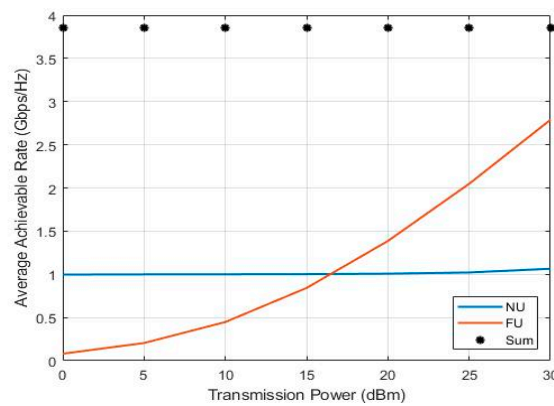


Figure 7. Achievable rate vs. transmit power.

### 5.3.2. Outage Probability against Transmit Power

As shown in Figure 8, the *FU* experiences a much greater outage than *NU* despite the larger (average) data rate in Figure 7 compared with *NU*, which is the normal performance according to their different conditions.

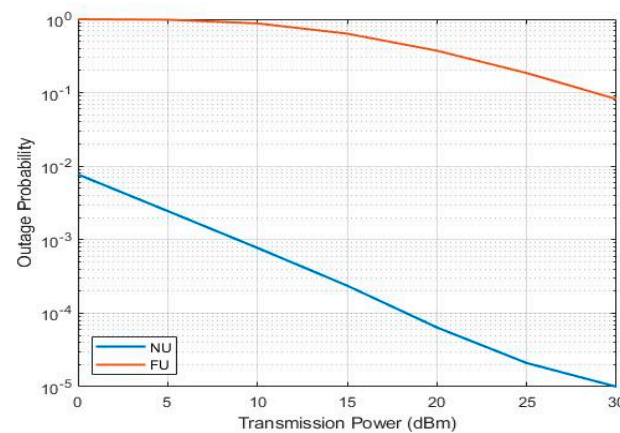


Figure 8. Outage probability vs. transmit power.

### 5.3.3. Instantaneous Rates

To study users’ performance accurately, we simulate instantaneous rates under channel realization.

In Figure 9, the *FU* still does not have better stability than the *NU* despite the higher data rate, and the *FU* instantaneous rate is pivoted around the same value it reached in Figure 7 with few spikes beneath the target rate. This condition explains the reasonable difference in outage performance between the two users.

In a brief comparison, our proposed system outperforms that of [23] in terms of simplicity, cost-effectiveness, computational complexity, SE, and EE. The system in [23] reaches our reference point (1 Gbps) by using more power (60 dBm), whereas we reached that point with only 17 dBm. Similarly, a data rate of only 1 Mbps is achieved at 20 dBm, where we achieve 1 Gbps for two users separately, showing the importance of the EH technique as a valuable contribution.

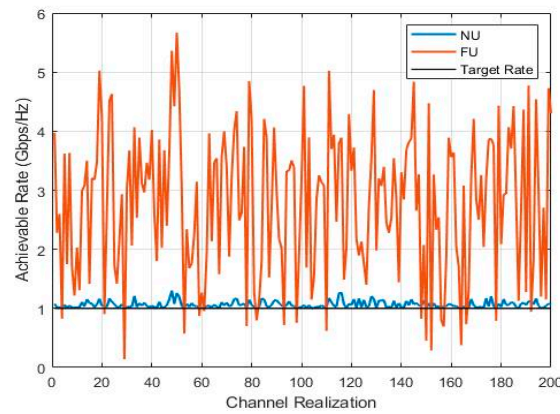


Figure 9. Instantaneous rate vs. channel realization.

#### 5.4. Scenario1 vs. Scenario2

In this section, we present the simulation of the main system model Scenario1 versus Scenario2 with its two cases in three subsections based on the parameters of Scenario1 and Scenario2 in Sections 4 and 5.

##### 5.4.1. Average Achievable Rate against Transmit Power

Figure 10 illustrates an observable difference between the two scenarios and how our main Scenario1 outperforms Scenario2 at NU and FU despite setting better parameters' values to Scenario2 (lower frequency, wider BW, and much power). On the one hand, in Scenario1, NU is saturated at the target rate immediately, and FU is met at the NU at 17 dBm power, where the NU with a longer BS-NU distance is saturated using 1.4 dBm power, and the FUs of Scenario2 are met at their NUs using 31 dBm power. All Scenarios' FUs data rates still increase exactly as explained in Figure 7. On the other hand, the enlarged BS-NU distance case shows more transmission effect than the enlarged NU-FU distance case by comparing the two cases in Scenario2.

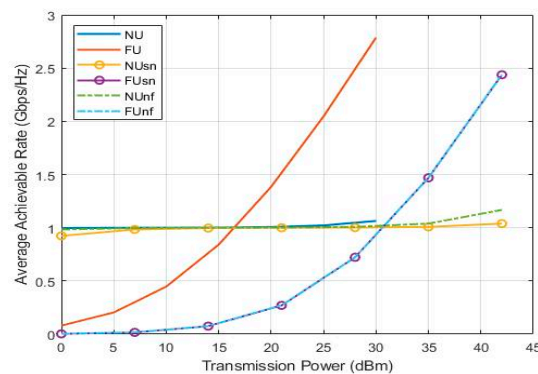
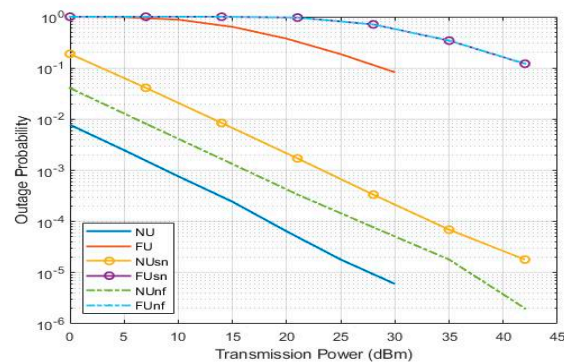


Figure 10. Achievable rate vs. transmit power.

##### 5.4.2. Outage Probability against Transmit Power

In outage probability comparison, Figure 11 depicts how our main scenario outperforms Scenario2 in NU and FU despite setting better parameters' values to Scenario2 (lower frequency, wider BW, and much power). On the one hand, in Scenario1, NU and FU show better outage performance than NU and FUs of Scenario2. On the other hand, the enlarged BS-NU distance case shows more transmission effect than the enlarged NU-FU distance case, regarding NU's outage performance by comparing the two cases in Scenario2. This condition is because the NU with a longer BS-NU distance outage probability is longer than that of a longer NU-FU distance.



**Figure 11.** Outage probability vs. transmit power.

#### 5.4.3. Instantaneous Achievable Rates

To study users' performance accurately in all scenarios, we simulated instantaneous achievable rates under channel realization.

As shown in Figure 12, our main scenario outperforms Scenario2 in the *NU* and the *FU* despite setting better parameters' values to Scenario2 (lower frequency, wider BW, and much power) in terms of *NU*'s stability and *FU*'s fluctuation spikes. On the one hand, in Scenario1, *NU* and *FU* show better performance than *NU* and *FUs* of Scenario2. On the other hand, similar to the results in Figure 9, the enlarged *BS-NU* distance case shows more transmission effect than the enlarged *NU-FU* distance case, regarding *NUs*' stability and *FUs*' fluctuating spikes below the target rate by comparing the two cases in Scenario2.

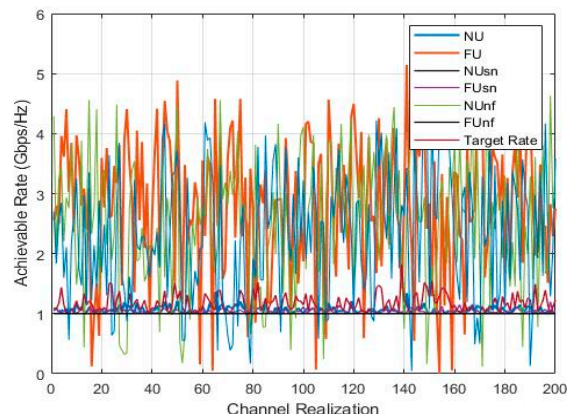


**Figure 12.** Instantaneous rate vs. channel realization.

The results of Section 5.4. demonstrate the importance of selecting the nearest user to the *Bs* to be *DF* relay because the *BS* signal is logically the dominant controller in *NOMA* power allocation, unlike signal that is transmitted by any *DF* relay while it harvests energy from *BS* and other surrounding sources, using that power for data retransmission for longer distance.

## 6. Challenges

The lack of THz equipment and resources (due to the circumstances of COVID-19 and its consequences across the world) is the biggest challenge that prevents us from conducting further verifications that we hope to provide as soon as possible. Moreover, despite the several advantages of the cooperative SWIPT THz-NOMA system over conventional systems, some challenges still need to be reconsidered. The most important one is mobility, especially with the increasing number of served users; hence, other metrics are affected by mobility such as CSI, power allocation, hardware limitation, beam steering, interference cancelation, and other related parameters; however, incorporating AI will improve CSI, localization, tracking, power allocation, and system performance.

## 7. Conclusions

THz communications, NOMA, and other emerging technologies have come into view to leverage the performance of the next era's wireless communications and networks; however, there are still some inevitable shortages that need to be solved, e.g., THz transmission distance due to its characteristics such as susceptibility to blockages. This paper starts with a brief comparison of DF relaying versus IRS, addressing the benefits, i.e., reduction in complexity and cost in addition to its suitability to open areas transmission media. The application of EH to the cooperative THz-NOMA system model is thoroughly studied, deriving the optimal value of the EH coefficient to achieve the targeted SINR, data rates, and SE for NOMA users. The maximum EE using the EH technique is measured and compared, setting a reference point of 1 Gbps. The overall system performance presents an added value to (and outperforms) the current systems and similar works, including [23], providing better performance (SE and EE improved by 70%) and considering the simplicity with cost-effectiveness over those systems. The distancing effect (Scenario2) of each transmission phase apart (i.e., case 1:  $d_{sn} > d_{nf}$ , case 2:  $d_{sn} < d_{nf}$ ) is studied and compared with the main system model (Scenario1) in terms of the achievable rate and outage probability. The overall results show how the defined techniques manage to maintain ongoing communication between the BS and the blocked *FU* and how overall performance is improved perfectly. The numerical results show that the *BS-NU* distance has a higher effect than the *NU-FU* distance when adjusted, demonstrating the importance of selecting the nearest user to the BS as a DF relaying user, adopting the proposed technologies.

For system planning, assuming that UDHNs are deployed with many distributed BSs, APs, relays, repeaters, and cooperatively user-relaying points, the proposed system can adapt with the connection failures cases, e.g., a terrestrial open space (or other shortage-based issues) where THz-NOMA smallest single-cell downlink transmission with a cluster of two paired users (as a representation of users in a cluster that will potentially be used in the future within a multi-clustered multicarrier hybrid THz-NOMA system).

**Author Contributions:** Conceptualization, H.W.O.; supervision, H.A.-R. All authors have read and agreed to the published version of the manuscript.

**Funding:** This research was funded by [Brunel University London].

**Conflicts of Interest:** The authors declare no conflict of interest.

## References

1. Han, S.; Xie, T.; Chih-Lin, I. Greener Physical Layer Technologies for 6G Mobile Communications. *IEEE Commun. Mag.* **2021**, *59*, 68–74. [[CrossRef](#)]
2. Jiang, W.; Han, B.; Habibi, M.A.; Schotten, H.D. The road towards 6G: A comprehensive survey. *IEEE Open J. Commun. Soc.* **2021**, *2*, 334–366. [[CrossRef](#)]
3. Alsabah, M.; Naser, M.A.; Mahmmod, B.M.; Abdulhussain, S.H.; Eissa, M.R.; Al-Baidhani, A.; Noordin, N.K.; Sait, S.M.; Al-Utaibi, K.A.; Hashim, F. 6G Wireless Communications Networks: A Comprehensive Survey. *IEEE Access* **2021**, *9*, 148191–148243. [[CrossRef](#)]
4. De Alwis, C.; Kalla, A.; Pham, Q.V.; Kumar, P.; Dev, K.; Hwang, W.J.; Liyanage, M. Survey on 6G Frontiers: Trends, Applications, Requirements, Technologies and Future Research. *IEEE Open J. Commun. Soc.* **2021**, *2*, 836–886. [[CrossRef](#)]
5. Akyildiz, I.F.; Kak, A.; Nie, S. 6G and Beyond: The Future of Wireless Communications Systems. *IEEE Access* **2020**, *8*, 133995–134030. [[CrossRef](#)]
6. Liu, Y.; Liu, F.; Zhu, G.; Wang, X.; Jiao, Y. Dynamic power optimization of pilot and data for downlink OFDMA systems. *J. Commun. Netw.* **2021**, *23*, 1–10. [[CrossRef](#)]
7. Rappaport, T.S.; Xing, Y.; Kanhere, O.; Ju, S.; Madanayake, A.; Mandal, S.; Alkhateeb, A.; Trichopoulos, G.C. Wireless communications and applications above 100 GHz: Opportunities and challenges for 6g and beyond. *IEEE Access* **2019**, *7*, 78729–78757. [[CrossRef](#)]
8. Chatzimisios, P.; Soldani, D.; Jamalipour, A.; Manzalini, A.; Das, S.K. Special issue on 6G wireless systems. *J. Commun. Netw.* **2020**, *22*, 440–443. [[CrossRef](#)]
9. Darsena, D.; Gelli, G.; Verde, F. Design and performance analysis of multiple-relay cooperative MIMO networks. *J. Commun. Netw.* **2019**, *21*, 25–32. [[CrossRef](#)]
10. Sun, Y.; Cyr, B. Sampling for data freshness optimization: Non-linear age functions. *J. Commun. Netw.* **2019**, *21*, 204–219. [[CrossRef](#)]

11. Gür, G. Expansive networks: Exploiting spectrum sharing for capacity boost and 6G vision. *J. Commun. Netw.* **2020**, *22*, 444–454. [[CrossRef](#)]
12. Elayan, H.; Amin, O.; Shihada, B.; Shubair, R.M.; Alouini, M.S. Terahertz band: The last piece of rf spectrum puzzle for communication systems. *IEEE Open J. Commun. Soc.* **2020**, *1*, 1–32. [[CrossRef](#)]
13. Sareddeen, H.; Alouini, M.S.; Al-Naffouri, T.Y. An Overview of Signal Processing Techniques for Terahertz Communications. *Proc. IEEE* **2021**, *109*, 1628–1665. [[CrossRef](#)]
14. Tataria, H.; Shafi, M.; Molisch, A.F.; Dohler, M.; Sjolund, H.; Tufvesson, F. 6G Wireless Systems: Vision, Requirements, Challenges, Insights, and Opportunities. *Proc. IEEE* **2021**, *109*, 1166–1199. [[CrossRef](#)]
15. Krishnamoorthy, A.; Schober, R. Uplink and Downlink MIMO-NOMA with Simultaneous Triangularization. *IEEE Trans. Wirel. Commun.* **2021**, *20*, 3381–3396. [[CrossRef](#)]
16. Liu, Y.; Yi, W.; Ding, Z.; Liu, X.; Dobre, O.; Al-Dhahir, N. Developing NOMA to Next Generation Multiple Access (NGMA): Future Vision and Research Opportunities. *arXiv* **2021**, arXiv:2103.02334.
17. Maraqa, O.; Rajasekaran, A.S.; Al-Ahmadi, S.; Yanikomeroglu, H.; Sait, S.M. A Survey of Rate-Optimal Power Domain NOMA with Enabling Technologies of Future Wireless Networks. *IEEE Commun. Surv. Tutor.* **2020**, *22*, 2192–2235. [[CrossRef](#)]
18. Liaqat, M.; Noordin, K.A.; Abdul Latef, T.; Dimiyati, K. Power-domain non orthogonal multiple access (PD-NOMA) in cooperative networks: An overview. *Wirel. Netw.* **2020**, *26*, 181–203. [[CrossRef](#)]
19. Ng, D.W.K.; Duong, T.Q.; Zhong, C.; Schober, R. *Wireless Information and Power Transfer: Theory and Practice*; John Wiley & Sons: Hoboken, NJ, USA, 2018.
20. Bjornson, E.; Ozdogan, O.; Larsson, E.G. Intelligent Reflecting Surface Versus Decode-and-Forward: How Large Surfaces are Needed to Beat Relaying? *IEEE Wirel. Commun. Lett.* **2020**, *9*, 244–248. [[CrossRef](#)]
21. Zhang, H.; Zhang, H.; Liu, W.; Long, K.; Dong, J.; Leung, V.C.M. Energy Efficient User Clustering, Hybrid Precoding and Power Optimization in Terahertz MIMO-NOMA Systems. *IEEE J. Sel. Areas Commun.* **2020**, *38*, 2074–2085. [[CrossRef](#)]
22. Saad, M.; Al Akkad, N.; Hijazi, H.; Al Ghouwayel, A.C.; Bader, F.; Palicot, J. Novel MIMO technique for wireless terabits systems in Sub-THz Band. *IEEE Open J. Veh. Technol.* **2021**, *2*, 125–139. [[CrossRef](#)]
23. Elkharbotly, O.; Maher, E.; El-Mahdy, A.; Dressler, F. Optimal power allocation in cooperative MIMO-NOMA with FD/HD relaying in THz communications. In Proceedings of the 2020 9th IFIP International Conference on Performance Evaluation and Modeling in Wireless Networks (PEMWN), Berlin, Germany, 1–3 December 2020.
24. IEEE. *IEEE Standard for High Data Rate Wireless Multi-Media Networks—Amendment 2: 100 Gb/s Wireless Switched Point-to-Point Physical Layer*; IEEE: Piscataway, NJ, USA, 2017; Volume 2017, ISBN 9781504442466.
25. Petrov, V.; Kurner, T.; Hosako, I. IEEE 802.15.3d: First Standardization Efforts for Sub-Terahertz Band Communications toward 6G. *IEEE Commun. Mag.* **2020**, *58*, 28–33. [[CrossRef](#)]